Electronic Properties of the Biphenylene Sheet and Its One-Dimensional Derivatives

Mathew A. Hudspeth,† Brandon W. Whitman,† Veronica Barone,* and Juan E. Peralta

Department of Physics, Central Michigan University, Mt. Pleasant, Michigan 48859. †These authors contributed equally to this work.

ABSTRACT We have studied the electronic properties and relative stability of the biphenylene sheet composed of alternating eight-, six- and four-carbon rings and its one-dimensional derivatives including ribbons and tubes of different widths and morphologies by means of density functional theory calculations. The two-dimensional sheet presents a metallic character that is also present in the planar strips with zigzag-type edges. Armchair-edged strips develop a band gap that decreases monotonically with the ribbon width. The narrowest armchair strip considered here (0.62 nm wide) presents a large band gap of 1.71 eV, while the 2.14 nm wide armchair strip exhibits a band gap of 0.08 eV. We have also found that tubes made by rolling these ribbons in a seamlessly manner are all metallic, independent of their chirality. However, while the calculated energy landscape suggests that planar strips present a relative stability comparable to that of C_{60}, in the tubular form, they present a more pronounced metastable nature with a Gibbs free energy of at least 0.2 eV per carbon higher than in C_{60}.

KEYWORDS: biphenylene · carbon material · carbon nanostructure · electronic structure · density functional theory

Low-dimensional carbon allotropes have received a lot of attention due to their unique properties. Fullerenes and carbon nanotubes have been extensively investigated due to their potential for electronic devices at the nanometer scale as well as their ability to encapsulate foreign atoms or molecules with likely applications in drug delivery.[1−4] These materials also present unique mechanical properties, arising from the strong covalent bonds forming the carbon network.[4,5]

More recently, one of the simplest forms of carbon, a two-dimensional honeycomb lattice dubbed graphene, has been synthesized in the lab.[6,7] This carbon network has been manipulated to form quasi-one-dimensional strips, graphene nanoribbons (GNRs), with tunable electronic properties that depend strictly on their geometry similar to the case of single-walled carbon nanotubes (SWNTs).[8−10] It is clear now that carbon nanomaterials present a huge versatility that can be exploited by controlling their structure at the atomic level.

In the quest of optimizing the electronic properties of nanocarbons for specific applications, other nongraphitic all-carbon networks and their low-dimensional derivatives have been proposed. For instance, Crespi *et al.* have shown that creation of defects in the honeycomb lattice can provide a metallic sheet with high density of states around the Fermi level.[11] Following this work, Terrones *et al.* proposed the Haeckelites and nanotubes made by rolling them in a seamless manner, as a new carbon allotrope with well-defined metallic behavior.[12] Although the predicted stability of these carbon networks is comparable to that of fullerenes,[12] their synthesis has been suggested to rely on the production of defects in the hexagonal lattice in a controllable and uniform way. This has proven to be a complicated task and prevents the production of such interesting all-metallic carbon structures.

Another two-dimensional carbon network based on the biphenylene dimer (Figure 1d) has been hypothesized, and their polymeric one-dimensional counterparts have been explored to some extent.[13−15] Importantly, the biphenylene dimer molecule has been synthesized using organic chemistry methods.[15,16]

In this work, the biphenylene sheet, composed of alternating eight-, six-, and four-carbon rings, and their one-dimensional derivatives, including ribbons and tubes of different widths and chiralities, are investigated by performing first-principles calculations based on density functional theory to explore their electronic structure and shed light on their relative stability.

RESULTS

Biphenylene Sheet and Planar One-Dimensional Derivatives. In Figure 1, we present a scheme of the various materials studied in this work.

*Address correspondence to v.barone@cmich.edu.

Received for review April 14, 2010 and accepted July 15, 2010.

Published online July 29, 2010. 10.1021/nn100758h

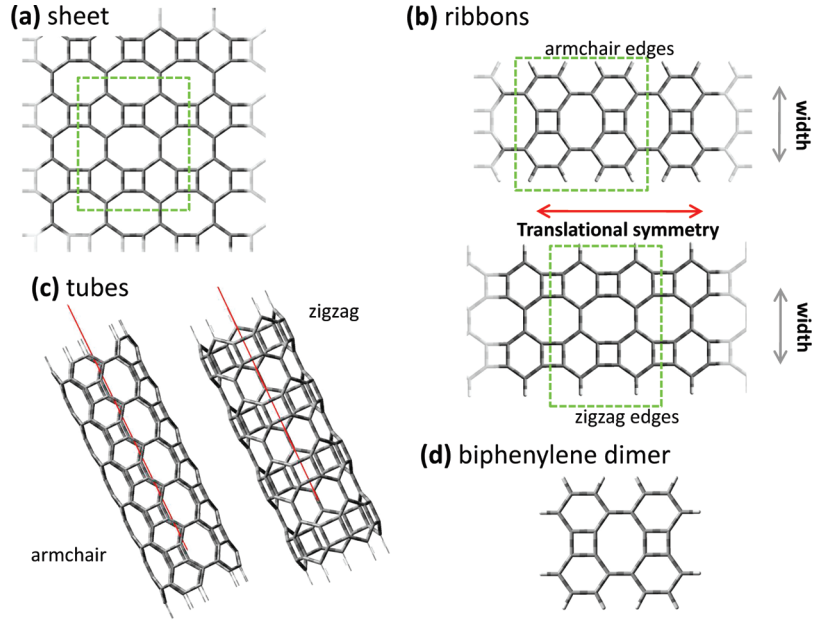

Figure 1. Scheme of the biphenylene sheet (a), its one-dimensional planar (b) and tubular (c) derivatives, and the biphenylene molecule (d) studied in this work.

The geometry of the two-dimensional biphenylene sheet is shown in Figure 1a. The limits of the unit cell employed in the calculations are marked by the dashed line. This unit cell is somewhat larger than the fundamental cell, thus allowing for more degrees of freedom during the geometry optimization. The optimized two-dimensional structure presents a metallic character manifested in the high density of states (DOS) at the Fermi level (set as zero), as shown in Figure 2.

To study the effect of quantum confinement in the biphenylene sheet, we consider quasi-one-dimensional ribbons with two different edge atomic connectivities and different widths. These polymers are represented in Figure 1b (in all cases, we consider hydrogen termination). In analogy to GNRs, these planar ribbons are dubbed *armchair* and *zigzag*, although for the zigzag case, the bonding at the edges is not equivalent to the corresponding bonding in GNRs. For each edge morphology, we consider five different ribbon widths, $w = 0.62$, 1.00, 1.38, 1.76, and 2.14 nm for the armchair configuration and 0.75, 1.20, 1.64, 2.09, and 2.54 nm for the zigzag. By cutting the biphenylene sheet into armchair strips, electronic confinement along the width produces a band gap opening. The narrowest armchair ribbon ($w = 0.62$ nm shown in Figure 1b) presents a large band gap of 1.71 eV. This band gap decreases monotonically as the width of the ribbon increases in such a way that the widest strip studied here, with $w = 2.14$ nm, presents a band gap of 0.08 eV. In Figure 3, we present the band structure and density of states of three armchair strips with widths of

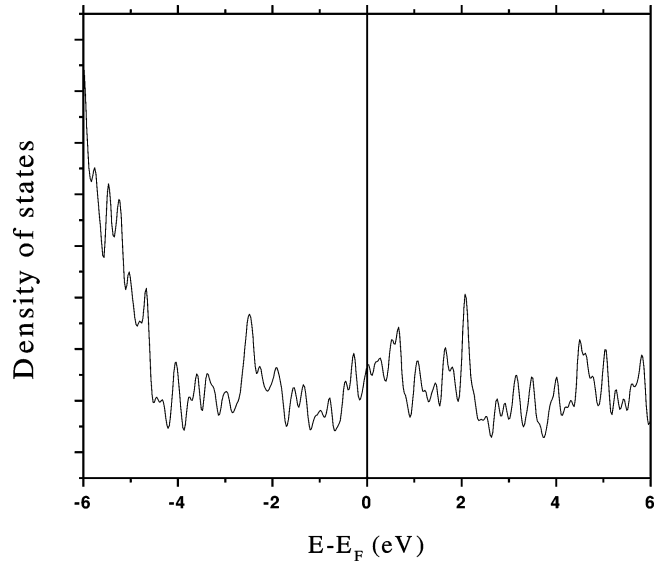

Figure 2. Density of states of the fully optimized biphenylene sheet obtained at the HSE/6-31G level.**

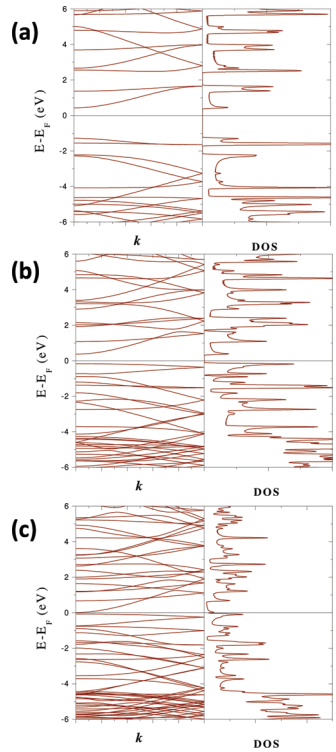

Figure 3. Band structure and density of states of planar armchair strips of different widths obtained at the HSE/6-31G level of theory. Widths shown here are (a) $w = 0.62$ nm, (b) $w = 1.38$ nm, and (c) $w = 2.14$ nm.**

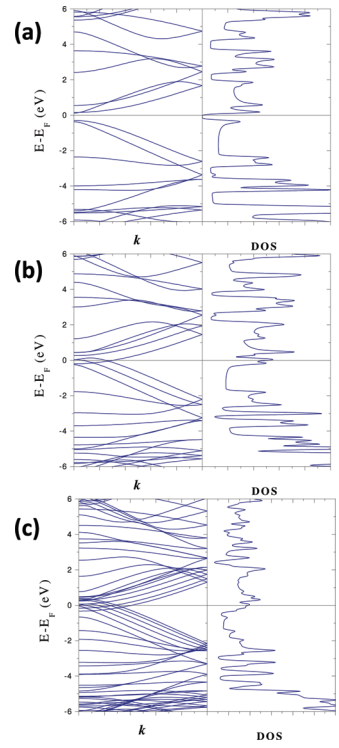

Figure 4. Band structure and density of states of planar zigzag strips of different widths obtained at the HSE/6-31G level of theory. Widths shown here are (a) $w = 0.75$ nm, (b) $w = 1.20$ nm, and (c) $w = 2.54$ nm.**

0.62, 1.38, and 2.14 nm, where the progressive band gap closing as w increases can be observed.

Now we turn to the discussion of the effect of the exchange-correlation functional on the electronic behavior of these systems. As mentioned above, the results presented here were obtained using the HSE functional. For comparison purposes, we have also performed these calculations with the generalized gradient approximation functional PBE, and we obtained a similar trend for the band structure than with HSE. However, PBE naturally underestimates the band gap in most cases, and therefore, we start observing a metallic behavior for the armchair strips at widths of about 1.38 nm, in contrast with the HSE results presented in Figure 3. As discussed above, this is a known difficulty of local and semilocal functionals, and therefore, the utilization of hybrid functionals in these systems is critical to obtain a reliable description of their electronic behavior.

For the zigzag configuration, we find a mostly metallic character except for the narrowest ribbon ($w = 0.75$ nm). This ribbon presents a band gap of about 0.4 eV. Larger width ribbons develop bands that cross the Fermi level (Figure 4). The number of bands crossing the Fermi level increases significantly with the ribbon width, producing an increasingly higher DOS at the Fermi level.

One of the striking properties of GNRs is the predicted magnetic behavior for the zigzag configuration.[17] This behavior could provide routes for designing spin-filters for spintronics applications. Although, as discussed earlier, the bonding of the "zigzag" configuration in the biphenylene strips does not correspond to the one in GNRs, we have studied the possibility of magnetism by performing spin-polarized calculations. These calculations (performed in both armchair and zigzag strips) resulted always in a spin-compensated

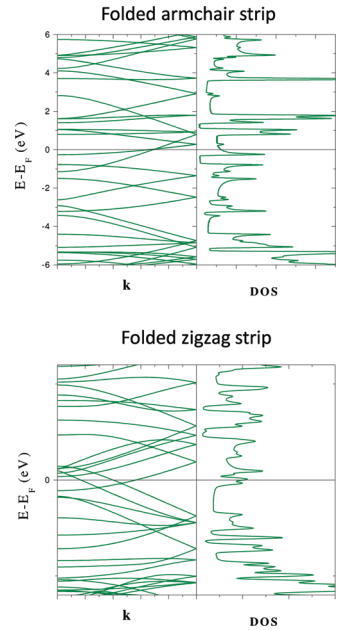

Figure 5. Band structure and density of states of tubes made by rolling the biphenylene strips obtained at the HSE/6-31G level of theory.**

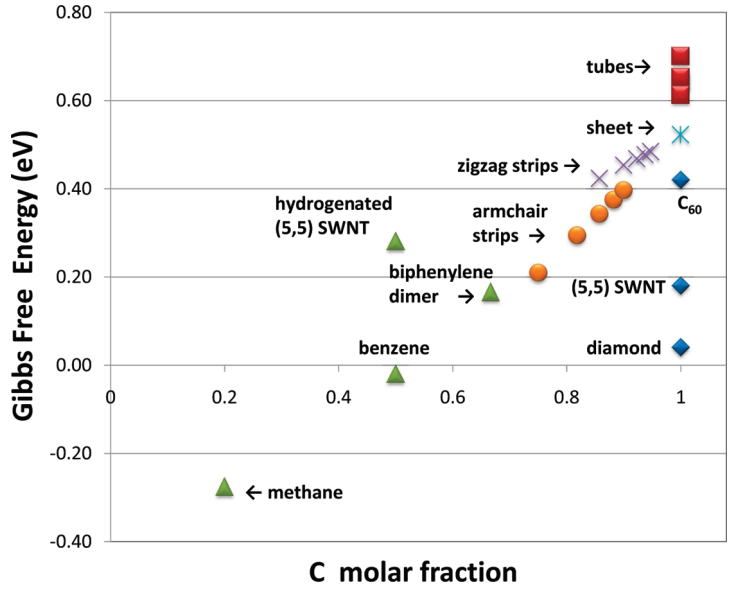

Figure 6. Relative stability of C-only and C−H compounds obtained at the HSE/6-31G level of theory. Negative values of δ*G* indicate stable structures with respect to its constituents (H_2 and graphene), while positive values indicate metastable structures. The star represents the two-dimensional sheet; cross and circles represent zigzag and armchair strips of different widths, respectively.**

ground state solution, which indicates the diamagnetic nature of the biphenylene polymers.

Tubes. By rolling these strips in a seamless way, it is possible to create tubular structures in analogy to the nonchiral armchair and zigzag single-walled carbon nanotubes but with a distinctive bonding. In the case of the tubes, both armchair (formed by folding zigzag strips) and zigzag (formed by folding armchair strips) present a metallic character with high DOS at the Fermi level (see Figure 5). Zigzag tubes exhibit a band structure similar to the armchair strips. However, curvature-induced hybridization produces a band that crosses the Fermi level, conferring these tubes the metallic character that is absent in the corresponding originating strips. Armchair tubes present the same trend as zigzag strips, with the number of bands crossing the Fermi level increasing as the diameter of the tube increases.

Energy Landscape. The strain imposed on the biphenylene molecule to the molecular structure by the four- and eight-membered ring makes it less stable than regular aromatic molecules.[18] It is therefore central to analyze the stability of the extended structures made out of the biphenylene dimer studied in this work. In order to do this, it is important to acknowledge that dangling bonds in the strips are passivated with H atoms, thus changing their chemical composition from all-carbon materials to hydrocarbons. Although formation energies are a way of studying the stability of the proposed materials, their meaningful comparison relies on the basis of identical chemical composition. Therefore, we need to adopt the approach customary for alloys and compute the Gibbs Free energy, δ*G*, of all the systems with respect to the natural forms of its constituents. In our case, as all the systems studied here are composed either of C or C and H, we compute δ*G* with respect to graphene and molecular hydrogen through the equation

$$\delta G(x) = E(x) + (1 - x_C)\mu_H + x_C\mu_C \qquad (1)$$

where $E(x)$ is the cohesive energy per atom of the system under consideration, x_C is the molar fraction of carbon atoms, and μ_H and μ_C are the chemical potentials of the constituents. We choose μ_H as the binding energy per atom of the H_2 molecule and μ_C as the cohesive energy per atom of a single graphene sheet.

Using eq 1, we compute δ*G* in these systems and present these values in Figure 6. For comparison purposes, we have included in this figure δ*G* for other molecules and extended structures such as single-walled carbon nanotubes, C_{60}, benzene, and the isolated biphenylene dimer, all optimized at the same level of theory. In Figure 6, we observe that, while the biphenylene sheet presents a δ*G* somewhat larger than fullerenes, their planar one-dimensional counterparts present a similar relative stability. The armchair configuration for the ribbons is more stable than the zigzag configuration. Tubes formed by rolling these strips are high in this energy landscape, indicating that they are less stable than their planar counterparts. δ*G* for the dimer is about the same as in the (5,5) SWNT and represents the lower limit of δ*G* for the planar strips.

CONCLUSIONS

We have studied the electronic properties and relative stability of the biphenylene sheet, composed of alternating eight-, six-, and four-carbon rings, and its one-dimensional derivatives, including ribbons and tubes of different widths and chiralities. Our DFT calculations show that the two-dimensional sheet presents a

metallic character that is also present in the planar strips with zigzag-type edges. Armchair-edged strips develop a band gap that decreases monotonically with the ribbon width. The narrow armchair ribbon (w = 0.62 nm) presents a large band gap of 1.71 eV, while a 2.14 nm wide armchair strip exhibits a band gap of 0.08 eV. Tubes made by seamlessly rolling these ribbons are all metallic, independent of their chirality. While planar strips present a relative stability comparable to that of C_{60}, tubes exhibit a more pronounced metastable nature with a δG that is at least 0.2 eV per carbon higher than in C_{60}.

METHODS

We have carried out all calculations utilizing a development version of the Gaussian suite of programs.[19] In this program, solid state calculations are performed using all-electron Gaussian basis sets and periodic boundary conditions imposed specifically in one, two, or three dimensions, depending on the dimensionality of the system under consideration.

Density functionals based on the local density approximation and the generalized gradient approximation predict Kohn−Sham gaps that severely underestimate experimental data, and often small gap semiconductors are erroneously predicted to be metallic. On the other hand, Kohn−Sham gaps from hybrid functionals (including a portion of Hartree−Fock type of exchange) are, in general, in better agreement with experimental gaps, although they tend to overestimate experimental data.[20−24] Screened exchange hybrid functionals improve upon regular hybrids and provide good agreement with experiments and more sophisticated many-electron approaches.[20,25−28] Therefore, we have chosen the screened exchange HSE funcional[29−31] and the double-ζ 6-31G** basis set[32] to perform the present study.

The reciprocal space integration has been performed in a 12 × 10 uniform k-point mesh per 9.0 × 7.5 Å^2 cell for the two-dimensional sheet and in a grid of 35 uniform k-point per 7.5 Å of translational vector for the one-dimensional derivatives. All of the structures have been fully relaxed until the maximum, and root-mean-square atomic forces are less than 0.02 and 0.015 eV/Å, respectively, and the maximum and root-mean-square atomic displacements between consecutive iterations are less than 10^{-3} and 6 × 10^{-4} Å, respectively.

Acknowledgment. V.B. acknowledges the donors of The American Chemical Society Petroleum Research Fund for support of this research through the award ACS PRF #49427-UNI6. J.E.P. acknowledges support from NSF DMR-0906617.

REFERENCES AND NOTES

1. Kinoshita, K. *Carbon, Electrochemical and Physicochemical Properties*; Wiley-Interscience: New York, 1987.
2. Saito, R.; Dresselhaus, G.; Dresselhaus, M. S. *Physical Properties of Carbon Nanotubes*; Imperial College Press: London, 1998.
3. Dresselhaus, M. S.; Dresselhaus, G.; Avouris, P. *Carbon Nanotubes: Synthesis, Structure, Properties and Applications (Topics in Applied Physics*; Springer: Heidelberg, 2001; Vol. 80.
4. Hu, J.; Odom, T.; Lieber, C. Chemistry and Physics in One Dimension: Synthesis and Properties of Nanowires and Nanotubes. *Acc. Chem. Res.* **1999**, *32*, 435–445.
5. Yakobson, B.; Avouris, P. Mechanical Properties of Carbon Nanotubes. *Top. Appl. Phys.* **2001**, *80*, 287–327.
6. Novoselov, K. S.; Geim, A. K.; Morozov, S. V.; Jiang, D.; Zhang, Y.; Dubonos, S. V.; Grigorieva, I. V.; Firsov, A. A. Electric Field Effect in Atomically Thin Carbon Films. *Science* **2004**, *306*, 666–669.
7. Berger, C.; Song, Z.; Li, X.; Wu, X.; Brown, N.; Naud, C.; Mayou, D.; Li, T.; Hass, J.; Marchenkov, A. N.; *et al.* Electronic Confinement and Coherence in Patterned Epitaxial Graphene. *Science* **2006**, *312*, 1191.
8. Wang, X.; Ouyang, Y.; Li, X.; Wang, H.; Guo, J.; Dai, H. Room-Temperature All-Semiconducting Sub-10-nm Graphene Nanoribbon Field-Effect Transistors. *Phys. Rev. Lett.* **2008**, *100*, 206803.
9. Han, M. Y.; Oezyilmaz, B.; Zhang, Y.; Kim, P. Energy Band-Gap Engineering of Graphene Nanoribbons. *Phys. Rev. Lett.* **2007**, *98*, 206805.
10. Kosynkin, D. V.; Higginbotham, A. L.; Sinitskii, A.; Lomeda, J. R.; Dimiev, A.; Price, B. K.; Tour, J. M. Longitudinal Unzipping of Carbon Nanotubes To Form Graphene Nanoribbons. *Nature* **2009**, *458*, 872–U5.
11. Crespi, V.; Benedict, L.; Cohen, M.; Louie, S. Prediction of a Pure-Carbon Planar Covalent Metal. *Phys. Rev. B* **1996**, *53*, 13303–13305.
12. Terrones, H.; Terrones, M.; Hernandez, E.; Grobert, N.; Charlier, J.; Ajayan, P. New Metallic Allotropes of Planar and Tubular Carbon. *Phys. Rev. Lett.* **2000**, *84*, 1716–1719.
13. Balaban, A. T. Carbon and Its Nets. *Comput. Math. Appl.* **1989**, *17*, 397–416.
14. Jr, K; M, M.; Hoffmann, R.; Balaban, A. T. 3,4-Connected Carbon Nets: Through-Space and Through-Bond Interactions in the Solid State. *J. Am. Chem. Soc.* **1987**, *109*, 6742–6751.
15. Rajca, A.; Safronov, A.; Rajca, S.; Ross, C. R.; Stezowski, J. J. Biphenylene Dimer. Molecular Fragment of a Two-Dimensional Carbon Net and Double-Stranded Polymer. *J. Am. Chem. Soc.* **1996**, *118*, 7272–7279.
16. Dosa, P. I.; Gu, Z.; Hager, D.; Karneyb, W. L.; Vollhardt, K. P. C. Flash-Vacuum-Pyrolytic Reorganization of Angular [4]Phenylene. *Chem. Commun.* **2009**, 1967–1969.
17. Son, Y.-W.; Cohen, M. L.; Louie, S. G. Half-Metallic Graphene Nanoribbons. *Nature* **2006**, *444*, 347–349.
18. Illuminati, G.; Mandolini, L. Ring Closure Reactions of Bifunctional Chain Molecules. *Acc. Chem. Res.* **1981**, *14*, 95–102.
19. Frisch, M. J.; Trucks, G. W.; Schlegel, H. B.; Scuseria, G. E.; Robb, M. A.; Cheeseman, J. R.; Montgomery, J. A., Jr.; Vreven, T.; Kudin, K. N. *et al. Gaussian*, Development Version (rev. f.1); Gaussian Inc.: Pittsburgh, PA, 2008.
20. Barone, V.; Peralta, J. E.; Wert, M.; Heyd, J.; Scuseria, G. E. Density Functional Theory Study of Optical Transitions in Semiconducting Single-Walled Carbon Nanotubes. *Nano Lett.* **2005**, *5*, 1621–1624.
21. Barone, V.; Peralta, J. E.; Scuseria, G. E. Optical Transitions in Metallic Single-Walled Carbon Nanotubes. *Nano Lett.* **2005**, *5*, 1830–1833.
22. Heyd, J.; Peralta, J.; Scuseria, G.; Martin, R. Energy Band Gaps and Lattice Parameters Evaluated with the Heyd−Scuseria−Ernzerhof Screened Hybrid Functional. *J. Chem. Phys.* **2005**, *123*, 174101.
23. Peralta, J. E.; Heyd, J.; Scuseria, G. E.; Martin, R. L. Spin−Orbit Splittings and Energy Band Gaps Calculated with the Heyd−Scuseria−Ernzerhof Screened Hybrid Functional. *Phys. Rev. B* **2006**, *74*, 073101.
24. Kümmel, S.; Kronik, L. Orbital-Dependent Density Functionals: Theory and Applications. *Rev. Mod. Phys.* **2008**, *80*, 3–60.
25. Batista, E. R.; Heyd, J.; Hennig, R. G.; Uberuaga, B. P.; Martin, R. L.; Scuseria, G. E.; Umrigar, C. J.; Wilkins, J. W. Comparison of Screened Hybrid Density Functional Theory to Diffusion Monte Carlo in Calculations of Total Energies of Silicon Phases and Defects. *Phys. Rev. B* **2006**, *74*, 121102.

26. Barone, V.; Hod, O.; Scuseria, G. E. Electronic Structure and Stability of Semiconducting Graphene Nanoribbons. *Nano Lett.* **2006**, *6*, 2748–2754.
27. Brothers, E. N.; Izmaylov, A. F.; Normand, J. O.; Barone, V.; Scuseria, G. E. Accurate Solid-State Band Gaps *via* Screened Hybrid Electronic Structure Calculations. *J. Chem. Phys.* **2008**, *129*, 011102.
28. Janesko, B. G.; Scuseria, G. E. Coulomb-Only Second-Order Perturbation Theory in Long-Range-Corrected Hybrid Density Functionals. *Phys. Chem. Chem. Phys.* **2009**, *11*, 9677–9686.
29. Heyd, J.; Scuseria, G. E.; Ernzerhof, M. Hybrid Functionals Based on a Screened Coulomb Potential. *J. Chem. Phys.* **2003**, *118*, 8207.
30. Heyd, J.; Scuseria, G. E.; Ernzerhof, M. Erratum: Hybrid Functionals Based on a Screened Coulomb Potential [*J. Chem. Phys. 118*, 8207 (2003)]. *J. Chem. Phys.* **2006**, *124*, 219924.
31. Heyd, J.; Scuseria, G. E. Assessment and Validation of a Screened Coulomb Hybrid Density Functional. *J. Chem. Phys.* **2004**, *120*, 7274.
32. This basis set consists of (3s2p1d) contracted Gaussian functions for C and Li and (2s 1p) for H.